Eur. Phys. J. B **15**, 177–185 (2000)

THE EUROPEAN PHYSICAL JOURNAL B

EDP Sciences

Finite-size effects in the self-organized critical forest-fire model

K. Schenk[1,a], B. Drossel[2], S. Clar[3], and F. Schwabl[1]

[1] Physik-Department der Technischen Universität München, James Franck Straße, 85747 Garching
[2] Theory Group, Department of Physics and Astronomy, University of Manchester, Manchester M13 9PL, UK
[3] iXOS Software AG, 85630 Grasbrunn, Germany

Received 24 April 1999 and Received in final form 26 October 1999

Abstract. We study finite-size effects in the self-organized critical forest-fire model by numerically evaluating the tree density and the fire size distribution. The results show that this model does not display the finite-size scaling seen in conventional critical systems. Rather, the system is composed of relatively homogeneous patches of different tree densities, leading to two qualitatively different types of fires: those that span an entire patch and those that do not. As the system size becomes smaller, the system contains less patches, and finally becomes homogeneous, with large density fluctuations in time.

PACS. 05.40.-a Fluctuation phenomena, random processes, noise, and Brownian motion – 05.70.Jk Critical point phenomena – 05.70.Ln Nonequilibrium and irreversible thermodynamics

1 Introduction

During the past years, systems which exhibit self-organized criticality (SOC) have attracted much attention, since they might explain part of the abundance of fractal structures in nature [1]. Their common features are slow driving or energy input and rare dissipation events which are instantaneous on the time scale of driving. In the stationary state, the size distribution of dissipation events obeys a power law, irrespective of initial conditions and without the need to fine-tune parameters. Examples for such systems are the sandpile model [1], the self-organized critical forest fire model [2,3], the earthquake model by Olami, Feder, and Christensen [4], and the Bak-Sneppen evolution model [5]. Numerical as well as analytical studies of those systems are usually based on the assumption that their critical behaviour can be described in similar terms as that of equilibrium critical systems. This assumption is given a basis in [6], where it is suggested that SOC systems can be mapped on conventional critical systems by interchanging control and order parameters. Thus, the Bak-Sneppen model can be mapped on a depinning problem [5]. However, it has been shown in [7] that the mapping suggested in [6] for the SOC forest-fire model does not generate a system with a conventional critical point. Instead, the phase transition shows hysteresis effects and is discontinuous when approached from above. Other unconventional features have also been seen in the SOC forest-fire model, like the existence of more than one diverging length scale [8,9], the absence of a spanning cluster immediately beyond the critical point [8], and the dependence of the large-scale behaviour on details of the model rules [9,10]. (For a review on the SOC forest-fire model, see [13].) Other SOC systems show also unconventional scaling behaviour. Thus, in the two-dimensional abelian sandpile model finite-size scaling is violated [14], and the critical exponents for the earthquake model by Olami, Feder, and Christensen [4] appear to depend continuously on the parameters. There is substantial need to better understand the nature of the scaling behaviour of those systems.

It is the purpose of this paper to shed some light on the unconventional critical behaviour of the SOC forest-fire model by studying its finite-size effects. We choose a version of the model which is identical to the SOC forest-fire model for system sizes much larger than the correlation length, and we discuss the changes that occur in the model as the system size is decreased below the correlation length. We find that instead of displaying finite-size scaling, small systems undergo a rearrangement from a structure with patches of different density to a more homogeneous structure with large density fluctuations in time. We find also that, contrary to conventional critical systems, small systems and small parts of large systems differ in the probability distribution for the density and in the fire-size distribution. We suggest that these results can be explained by the fact that the system has two qualitatively different types of fires.

The outline of this paper is as follows: in Section 2, we define the model that we used for studying finite-size effects, and discuss briefly known results. Section 3 shows computer simulation results for the fire-size distribution and the tree density as the system size changes from values larger than the correlation length to values much smaller

[a] e-mail: kschenk@ph.tum.de

than it. In the conclusion, we summarize and discuss our findings.

2 The model

The version of the SOC forest-fire model studied in this paper is defined on a square lattice with L^2 sites. Each site is either occupied ("tree") or empty ("no tree"). At each time step, the system is updated according to the following rules: (i) "Burning": a site in the system is chosen at random ("struck by lightning"). If the site is occupied, the whole cluster of occupied sites connected to this site (by nearest-neighbour coupling) is removed from the system ("burnt"), *i.e.*, the occupied sites of that cluster turn to empty sites. If the chosen site is empty, nothing happens. (ii) "Tree growth": we select randomly $s_0 \equiv pL^2$ sites from the system and occupy those that are empty (possibly also including sites which have become empty due to the removal of the cluster). These sites are selected one after another, allowing for the same site being selected more than once during the same filling step. In principle, s_0 can therefore be larger than L^2, however, in our simulations we chose usually values smaller than L^2.

For fixed s_0 and very large system size L, these rules are equivalent to having a lightning probability $f = 1/L^2$ per site and time step, and a tree growth probability p, and the model is identical to the original SOC forest-fire model [2]. Because of this equivalence, which was first pointed out by Grassberger [15] most numerical studies of the SOC forest-fire model up to now were performed using the above rules, which allow for fast and efficient computer simulations. With the above rules, finite-size effects can also be studied very efficiently, as was suggested in [9]. However, one has to keep in mind that the results are somewhat different from those for the original model. While in the original model lightning can strike the system between the growth of any two trees, it can strike the system in the present model only after growth step (ii) is finished. This leads to density peaks in Figures 10 and 11 below that are not present in the original model. However, our main conclusions are not affected by the particular choice of the dynamical rules, as will be discussed further below.

Let us first summarize shortly the major numerical results for the case $s_0 \ll L^2$, as reported in the literature on the SOC forest-fire model [3,15–17]. In this limit, only a small number of trees grow at each time step (compared to the total number of trees). After a transient time, a stationary state is reached where the tree density has only small fluctuations around some average value $\bar{\rho}(s_0)$ that does not depend on L. Throughout this paper, we study only stationary states and do not evaluate the initial transient behaviour. Since the mean number of trees $\bar{s}$ burnt during a fire must be identical to the mean number of trees growing between two fires, we have the relation

$$\bar{s} = s_0(1-\bar{\rho})/\bar{\rho}. \tag{1}$$

The leading finite-size corrections to this equation are of order s_0/L^2 and can be neglected in the case $s_0 \ll L^2$ which we are considering in this paragraph. As s_0 increases, the mean fire size increases also, and we approach the critical point of the SOC forest-fire model, where the mean tree density is given by $\bar{\rho}_c \simeq 0.41$. The correlation length ξ is a measure for the radius of the largest tree cluster and is related to s_0 via $\xi \sim s_0^{\nu}$, with $\nu \approx 0.58$ in $d = 2$ dimensions. The size distribution of tree clusters near the critical point is well-described by the scaling form

$$n(s) \simeq s^{-\tau}\mathcal{C}(s/s_{\max}), \tag{2}$$

with a cutoff function $\mathcal{C}$ that is constant for small arguments and decays exponentially fast when the argument is considerably larger than 1. The cutoff cluster size $s_{\max}$ is related to the correlation length ξ via $s_{\max} \sim \xi^{\mu}$, with μ being the fractal dimension of tree clusters, which is found to be 1.95 [16] or 1.96 [3,11]. The value of the exponent τ is approximately 2.14. The relation between $s_{\max}$ and s_0 is $s_{\max} \sim s_0^{\lambda}$, with $\lambda = \nu\mu \simeq 1.15$ [3].

All these numerical findings agree well with conventional scaling assumptions based on a single diverging length scale. Analytical studies of the model, such as mean-field theories [17–19] and renormalization group calculations [20,21] are also based on conventional scaling assumptions. Therefore, the violation of finite-size scaling described in the following might appear surprising to many readers. However, one must keep in mind that the simulation data do not cover much more than one decade in the correlation length ξ. The observed scaling behaviour equation (2), together with the measured values of the critical exponents, do not necessarily indicate an exact asymptotic scaling form, but may simply be a good approximation to more complicated scaling, which works well for the system sizes and parameter values studied in simulations. A similar phenomenon is known for the sandpile model, where good scaling collapses for the avalanche size distribution could be achieved in [22,23] and older papers, although it has been recently shown [14] that finite-size scaling is violated and that the simple scaling ansatz used for the data collapse is incorrect.

Figure 1 shows a snapshot of a system with a tree density $\bar{\rho}$ just below $\bar{\rho}_c$. One can distinguish regions of different densities with a rather homogeneous tree distribution within a region. These regions are obviously created by a fire that burns down a cluster of high tree density. After the fire, a burnt region is almost empty and becomes slowly filled with trees according to the law $\dot{\rho} = p(1-\rho)$. We call these regions of homogeneous tree density "patches", as we did in [25]. If lightning strikes a tree in a patch of low density, it usually burns down a small tree cluster. If it strikes a patch of a density larger than the percolation threshold, it burns down a tree cluster as large as the patch itself. This observation indicates that there are two qualitatively different types of fires in the system: those that span an entire patch, and those that destroy a small percolation cluster within a patch of a tree density below the percolation threshold. As we will see below, this gives rise to the unusual finite-size properties of the model.

If the correlation length ξ is of the same order as or larger than L, the behaviour sketched above is modified

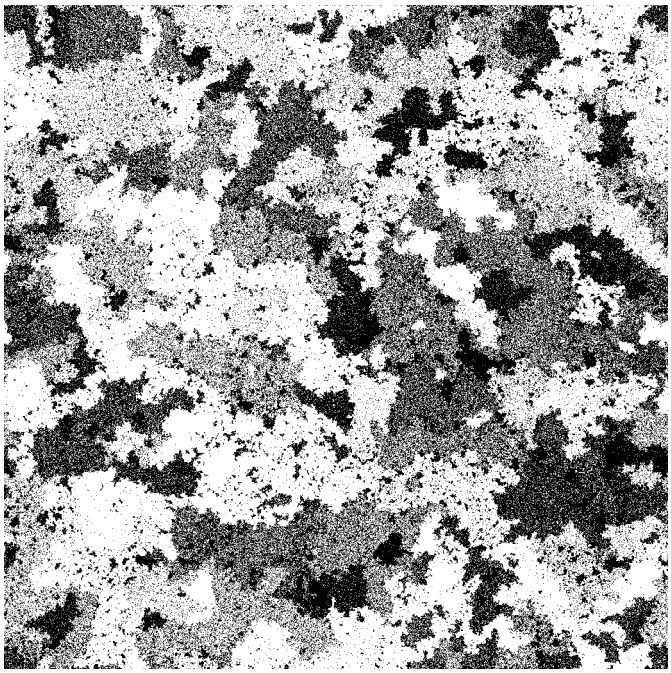

Fig. 1. Snapshot of the SOC forest-fire model for $\bar{\rho} \simeq \bar{\rho}_c \simeq 40.8\%$ and $L = 4096$. Trees are black and empty sites are white.

due to finite-size effects. For not too small values of s_0/L^2, the tree density increases by a noticeable amount between two fires, leading to large density fluctuations and to fires that span the entire system. If the SOC forest-fire model showed conventional critical behaviour, there would be a single diverging length scale, namely the correlation length ξ, which would be related to f/p or, equivalently, to s_0, via $\xi \sim (f/p)^{-\nu}$ or $\xi \sim s_0^{\nu}$. Finite-size effects would then manifest themselves in a scaling form

$$n(s) \simeq s^{-\tau} \mathcal{C}(s/L^{\mu}), \tag{3}$$

for the size distribution of tree clusters. Furthermore, on scales smaller than L and ξ, all measured quantities should be indistinguishable from those measured in a small section of an infinitely large critical system.

The following section presents simulation results that show that none of these finite-size scaling assumptions is satisfied for the SOC forest-fire model. In fact, the invalidity of the assumption of a single diverging length scale has already been shown in [9]. The invalidity of the second assumption that measurements in small systems and in small sections of large systems should give identical results, can be understood by considering for instance the mean time interval between two fires. In a small subsystem of linear size l of a large system with a correlation length $\xi \gg l$, this is given by $(p(1-\bar{\rho}_c))^{-1}$. Just before fire reaches the subsystem, its tree density is far above the percolation threshold, and the spanning cluster of the subsystem is part of a large tree cluster that extends far beyond the limits of the subsystem. Lightning usually strikes this large cluster outside the subsystem, the time interval between two lightning strokes within the subsystem being L^2/l^2, which diverges as L diverges. In contrast, fire cannot enter a small system from outside, but the tree density of a small system increases until lightning strikes a tree within the system. According to our rules, time is measured in units of the mean time interval between two lightning strokes. On this time scale, the time between two fires within a small system of linear size l is finite. In contrast, the time interval between two fires within a subsystem of size l of a much larger system is vanishingly small compared to the time interval between two lightning strokes within the subsystem. All these arguments are backed up and complemented by the numerical results reported in the following.

3 Results of computer simulations

In this section we will present and explain data obtained from about 300 runs of the model for various values of s_0 and L. Since many runs of the simulation were necessary, we chose a cluster of workstations rather than a "supercomputer". The system size L varied between 10 and 2000 in these runs. We found that as finite-size effects become more important, the system shows a transition between two qualitatively different types of behaviour which we call critical behaviour and percolation-like behaviour. The critical behaviour is is characterized by a good scaling collapse of the fire size distribution and by large spatial variations in the local tree density. The percolation-like behaviour is characterized by large temporal fluctuations in the global tree density, with a rather homogeneous tree distribution within the system for any given time. Snapshots of the system therefore resemble percolation systems where each site is occupied by a tree with a probability ρ. (For an introduction to percolation theory, see *e.g.* [24].) The following three subsections show how this transition manifests itself in the mean tree density, the fire size distribution, and the probability distribution for the tree density.

3.1 Lines of constant tree density

First, we measured the mean tree density

$$\bar{\rho} = (1/T) \sum_{t=1}^{T} \rho(t) \tag{4}$$

in the system, averaged over a large number of T iterations, for various values of L and s_0. The density $\rho(t)$ was always evaluated after the refilling step (ii). Compared to a model where trees grow at a rate $\dot{\rho} = p(1-\rho)$, the density values in our model are somewhat larger when s_0/L^2 is not very small. If, for instance, the density is increased from $\rho - \Delta\rho$ to ρ during the refilling step (ii), the value ρ enters the above sum, while an evaluation based on a constant growth rate would give $1 - \Delta\rho/\ln(1+\Delta\rho/(1-\rho))$ instead of ρ.

It it not obvious what the relation between s_0, L^2 and $\bar{\rho}$ should be if we want to deduce it from an analogy with

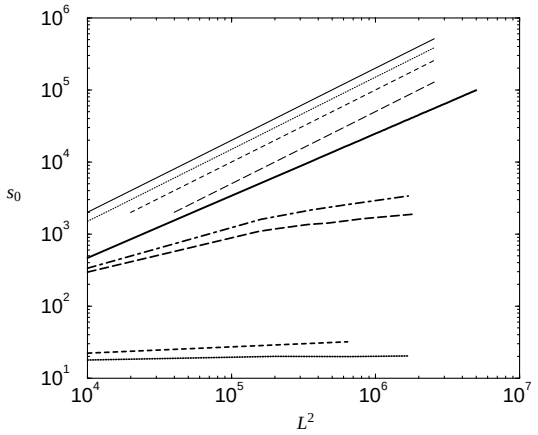

Fig. 2. Lines of constant mean tree density in a s_0 *vs.* L^2 plane. The bold solid line represents the separatrix between the SOC and the percolation-like behaviour. The remaining lines represent constant $\bar{\rho} = 0.47$, 0.455, 0.43, 0.42, 0.0403, 0.40, 0.35, 0.343 (from top to bottom). The line for $\bar{\rho} = 0.40$ is derived from interpolated results.

equilibrium critical systems. We have already mentioned that the temporal fluctuations in $\rho(t)$ become larger as the ratio s_0/L^2 increases. Similarly, temporal fluctuations increase in a critical equilibrium system when the system size becomes smaller. One might therefore expect that decreasing L at fixed s_0 should drive the system toward the critical point, where $\bar{\rho} = \bar{\rho}_c \simeq 0.41$. However, we have argued in the previous section that a given site burns down more often in a large system without finite-size effects than in a smaller system with finite-size effects that has the same value of s_0. From this, it follows that the mean tree density increases with decreasing L, when s_0 is fixed. In the limit $s_0 \gg L^2$ it must go to one. From this point of view, a system with sufficiently large finite-size effects should rather be compared to an equilibrium system in the ordered phase, for instance to a percolation system beyond the percolation threshold. The analogue of s_0 in a percolation system is then the mean size of the cluster that a given site belongs to, and it is proportional to L^2 beyond the percolation threshold [24]. Indeed, we find that the mean size of fires becomes proportional to L^2 when finite-size effects are strong (see below). However, there is nevertheless a fundamental difference between a percolation system beyond the percolation threshold and our system with a density above ρ_c: In our model, a tree cluster that spans the system and has a size proportional to L^2 occurs only rarely when the mean density is only slightly above the critical density, while a percolation system above the percolation threshold has always a system spanning tree cluster.

In Figure 2, lines of constant mean tree density are plotted on a double logarithmic scale in s_0 and L^2. This figure shows that there are two qualitatively different regions in the s_0 *vs.* L^2 plane, with a transition region between them. First, there is the region where there are no finite-size effects, $s_0 \ll L^2$. In this region, the size of the tree clusters is much smaller than the system size, and the global density fluctuations are small. The mean tree density of such a system is smaller than $\bar{\rho}_c \approx 0.41$. For systems with small density fluctuations the probability that a given empty site is filled with a tree during one time step, is given by s_0/L^2, and the probability that a given tree is burnt by a fire is $s_0(1-\bar{\rho})/(\bar{\rho}L^2)$. Since both probabilities decrease as $1/L^2$ with increasing L, dynamics of larger systems are slower than those of smaller systems. Apart from this change of the characteristic time scales, the local dynamics is independent of L, and consequently correlation functions and cluster size distributions are the same for systems of different sizes (provided that $L^2 \gg s_0$). This leads to the horizontal slope in the large L regime of the curves for $\bar{\rho} < \bar{\rho}_c$ in Figure 2.

The curves show deviations from the horizontal behaviour when L becomes as small as or smaller than the correlation length $\xi \sim s_0^\nu$. These deviations occur in the transition region where finite-size effects begin to become noticeable. The dynamics changes from fires that are not affected by the finite system size to a fire size distribution that includes sometimes events of the order of the system size. Fires of such a large size destroy the patchy structure of the forest described earlier, and cause a more random tree distribution.

In the second region, lines of constant mean density are curves of constant s_0/L^2. This feature can best be understood when considering the parameter range where s_0 is of the order of L^2 or above. In this range, the mean tree density is much larger than $\bar{\rho}_c$, and the system contains a spanning cluster after each filling. During the "burning" step, this cluster is removed with a finite probability, leading to a large change in density in the system. When a "finite" (*i.e.* not spanning) cluster is removed during the "burning" step, the overall density hardly changes for large L. The time series of the density is therefore determined almost completely by the filling events and by the large burning events. Since the filling events fill a large fraction of empty sites, and since large burning events burn a large fraction of trees, the tree distribution within the system is rather homogeneous. A snapshot of the system at a given time looks therefore similar to a percolation system with a density $\rho(t)$. From percolation theory we know that for a given density the fraction of trees sitting in the spanning cluster is independent of L, and consequently curves of constant large density are curves of constant s_0/L^2 in Figure 2. Even curves for smaller s_0/L^2, which correspond to densities only slightly above $\bar{\rho}_c$ show for sufficiently large L an asymptotic behaviour $s_0/L^2 =$ const, with the constant vanishing at $\bar{\rho}_c$. The reason is again that finite fires do not reduce the density of an infinitely large system, and that the system spanning fires reduce the density by an amount that does not depend on L, but only on the density itself.

Finally, the critical curve (for the density $\bar{\rho} = \bar{\rho}_c \simeq 0.41$) is obtained from the condition

$$L \approx \xi \sim s_0^\nu, \quad \text{with } \nu \simeq 0.58.$$

This curve is the separatrix between the two regions described above and is indicated in Figure 2 by the bold line.

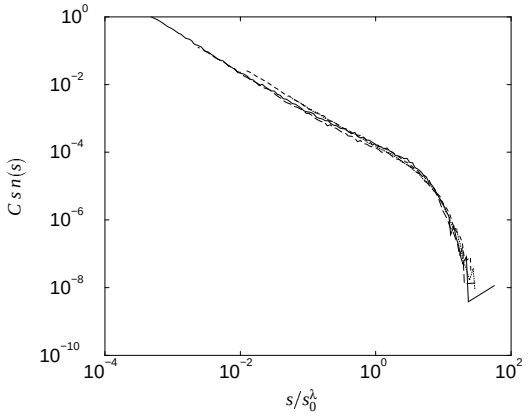

Fig. 3. Scaling collapse of the fire size distribution for systems with the parameters $s_0/L^2 = 0.001$ and $L = 1600$, 800, 400, 200. The measured mean tree densities are $\bar{\rho} = 0.40$, 0.395, 0.38, 0.36. C is a suitable scaling constant for each curve.

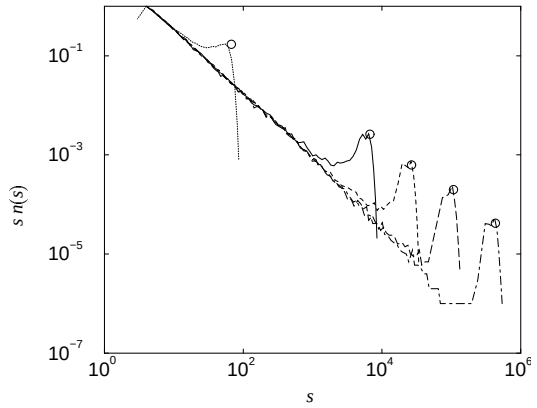

Fig. 4. The size distribution of fires for $s_0/L^2 = 0.15$ and $\bar{\rho} = 0.454$, for the system sizes $L = 10$, 100, 200, 400, 800 (as the peaks move from left to right). The circles mark the points of exact L^2 scaling, taking the peak of the $L = 800$ curve as reference.

As L decreases, more and more curves merge with the separatrix when their correlation length becomes comparable to the system size.

3.2 The fire size distribution

Since lightning strikes each tree with the same probability, the size distribution of fires is proportional to $sn(s)$, with $n(s)$ being the size distribution of tree clusters. As mentioned above, conventional scaling would imply a form $sn(s) \simeq s^{1-\tau}\mathcal{C}(s/s_0^{\mu\nu})$ for the fire size distribution if the correlation length $\xi \sim s_0^\nu$ is smaller than the system size, and a finite-size scaling form $sn(s) \simeq s^{1-\tau}\mathcal{C}(s/L^\mu)$ in the opposite case. In both cases, one would obtain a scaling collapse of the curves for different s_0 or L.

Figure 3 shows the fire size distribution for parameters such that $\xi < L$. While not perfect, the data collapse is good and would not impose the conclusion that simple scaling is violated. The bump near the end of the curves indicates that the cutoff function $\mathcal{C}$ increases first with increasing argument, before it shows the exponential decay. This bump is believed to contain all the trees that would sit in larger clusters if the system was exactly at the critical point [15].

Figure 4 shows the fire size distribution for parameter values such that the mean density is ten percent above its critical value. As discussed in the previous subsection, system spanning fires occur, and their size scales as L^2. These fires are responsible for the peaks in the fire size distribution. Similar peaks occur in equilibrium critical systems in the ordered phase, for example in the cluster size distribution of a percolation system above the percolation threshold. In a percolation system, the occurrence of such peaks implies that the system size is larger than the correlation length, which is identical to the cutoff in the radius of the finite (*i.e.*, non system spanning) clusters. In our system, however, we do not see such an exponential cutoff to the size distribution of the finite clusters. Instead, the curve for $L = 800$ in Figure 4 appears to obey a power law from $s \simeq 100$ up to the point where the peak begins. The explanation for this unusual behaviour must lie in the large temporal fluctuations in the density. The density is only sometimes so large that the large fires, which have a size of the order $L^2/2$, occur. At other times, the density values are different and allow for a broad range of other fire sizes.

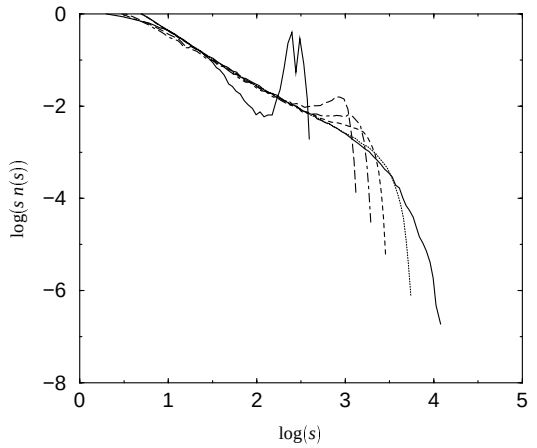

Fig. 5. Transition from critical to percolation-like behaviour as the system size L is decreased for the fixed parameter $s_0 = 200$. The parameter L of the curves are from right to left: $L = 1300$, 100, 63, 50, 40, 20. The measured mean tree densities are $\bar{\rho} =$ 0.385, 0.392, 0.402, 0.414, 0.432, 0.577.

The transition between critical scaling and L^2-scaling can be observed when L is varied for fixed s_0, as illustrated in Figure 5. One can see that the shape of the curves changes continuously as L is decreased. Clearly, because of this change in shape, finite-size effects do not manifest themselves in a scaling behaviour $sn(s) \simeq s^{1-\tau}\mathcal{C}(s/L^\mu)$. It is impossible to generate a scaling collapse of different curves, even if their density is close to the critical density. Furthermore, as mentioned above, the cutoff introduced

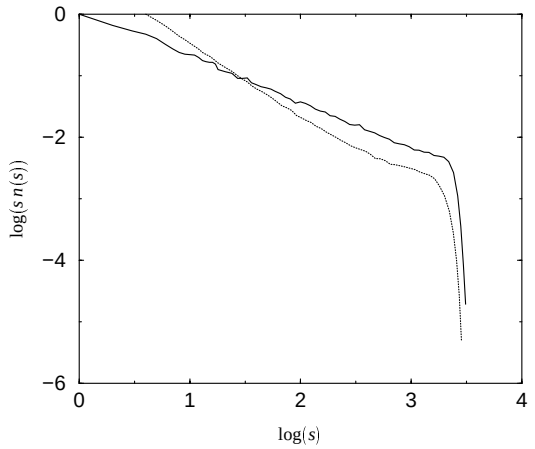

Fig. 6. Comparison of the fire size distribution of a section of size $l = 63$ of a larger ($L = 600$, $s_0 = 1440$) system (solid line) and a small system with $L = 63$ ($s_0 = 200$) (dotted line). For both systems we measured a mean tree density of $\bar{\rho} = 0.401$.

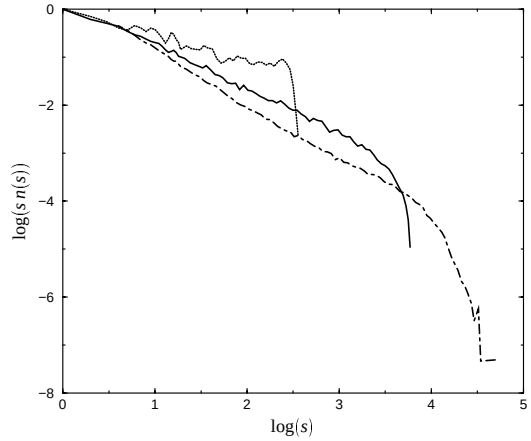

Fig. 7. Fire size distribution for systems with $L = 800$ (dot-dashed line) and of subsections of this system of size $l = 100$ (solid line) and $l = 20$. We used $s_0/L^2 = 0.001$ and measured the mean tree density $\bar{\rho} \approx 0.40$.

by the finite system size always scales as L^2, due to the occurrence of system spanning fires, and not as L^μ, as expected for conventional critical systems.

For small system sizes, spanning clusters may already occur for densities below $\bar{\rho}_c$, an effect which is clearly visible in the curve for $L = 63$. The formation of peaks due to finite size effects, was also found in [12].

As mentioned earlier, for conventional critical systems a system of small size and a small section of a large system are equivalent. We have argued that this is not true for the forest-fire model since the mean tree density and the time interval between fires are different in the two cases. The next two figures show that also the fire size distributions are different. In Figure 6 the fire size distribution of a section of a large system and a corresponding small system is shown. The scaling parts and the form of the bumps near the cutoff are very different. The fire size distribution of a small section of a large system is broader than that of a small system. The reason is that a section of a large system can contain a boundary between a patch of large tree density and a patch of small tree density. This boundary can pass through the section in different ways, and the number of trees in the dense part can take different values. Since large fires only burn the dense part, the size distribution of fires becomes broad.

Figure 7 shows how the fire size distribution changes when smaller and smaller sections of a large system are evaluated. In comparison with Figure 5, one sees again that the fire size distribution of small sections of large systems is different from that of small systems.

To summarize this subsection, the fire size distribution in the presence of finite-size effects does not show the features of finite-size effects in conventional critical systems. We find a continuous change in the shape of the fire size distribution and cutoffs that scale as L^2, rather than conventional finite-size scaling. Furthermore, the fire size distribution in small sections of large systems is different from small systems. Our results for the fire-size distribution confirm the qualitative transition from a parameter region unaffected by finite-size effects to a region dominated by system spanning fires that we found in the previous subsection.

3.3 Probability distribution of the density

Finally, we studied the temporal fluctuations in the values of tree density $\rho(t)$ by measuring how often a given value of ρ occurs within a sufficiently long time series. We denote by $w(\rho)\mathrm{d}\rho$ the probability that the tree density lies in the interval between ρ and $\rho + \mathrm{d}\rho$. The quantity $w(\rho)$ is therefore the probability density for the tree density ρ. We measured ρ always after the trees were refilled, *i.e.*, after step (ii). The results show again a qualitative change as the correlation length becomes smaller than the system size, reflecting the transition from critical to percolation-like behaviour.

In Figures 8 to 11 $w(\rho)$ is shown for different values for L and s_0. For large enough and fixed s_0/L^2, the mean tree density increases with increasing system size, until it reaches its asymptotic value above $\bar{\rho}_c$. For fixed L, the mean tree density increases with increasing s_0. Apart from this increase in mean tree density, the following other trends are observed: (a) as the mean density approaches $\bar{\rho}_c$, the curves for $w(\rho)$ become broader (Fig. 8). This is because the patches of homogeneous density visible in Figure 1 become larger with increasing $\bar{\rho}$, leading to larger global density fluctuations. (b) As the mean tree density increases above $\bar{\rho}_c$, the shape of the distribution becomes asymmetric, with the maximum moving from $\bar{\rho}_c$ to the percolation threshold $\rho_{\mathrm{perc}} \simeq 0.59$ (Fig. 9). The reason is that for $\bar{\rho} > \bar{\rho}_c$ the patchy structure is replaced by a more homogeneous (percolation like) structure, where the largest fires are system spanning and occur for densities above the percolation threshold. Once the density lies above the percolation threshold the probability that a system spanning fire occurs is very high. This is why densities

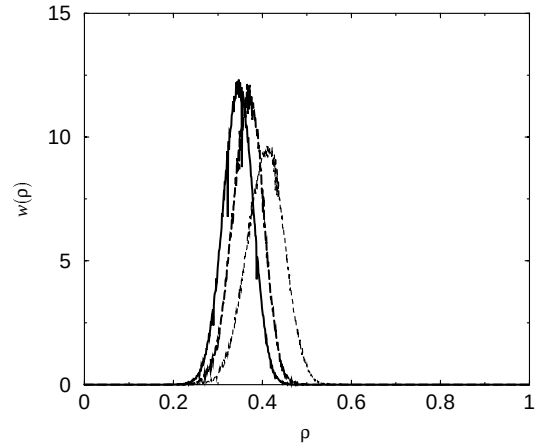

Fig. 8. $w(\rho)$ for systems with the parameters $s_0/L^2 = 0.005$ and $L = 63$, 100, 1600 (as the peaks move from left to right). The measured mean tree densities are $\bar{\rho} = 0.345$, 0.367, 0.407.

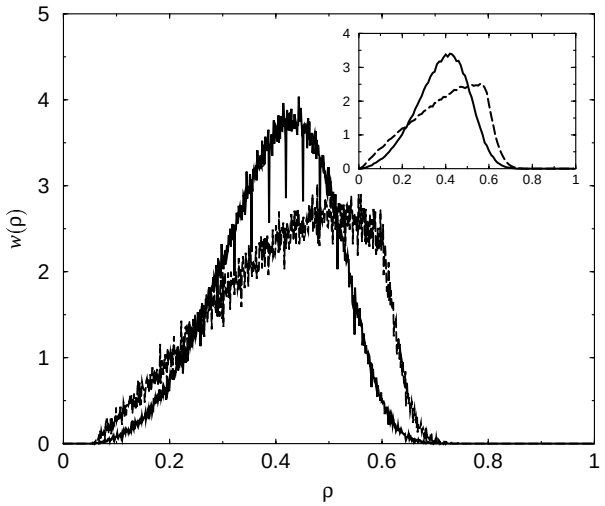

Fig. 9. $w(\rho)$ for systems with the parameters $s_0/L^2 = 0.05$ and $L = 63$, 1600 (as the peaks move from left to right). The measured mean tree densities are $\bar{\rho} = 0.402$ and 0.423. The inset shows $w(\rho)$ for the test simulation with an exponential probability distribution for s_0. The values of L, and the mean value of s_0 are the same as in the main figure, the measured mean tree densities are $\bar{\rho} = 0.39$ and 0.408.

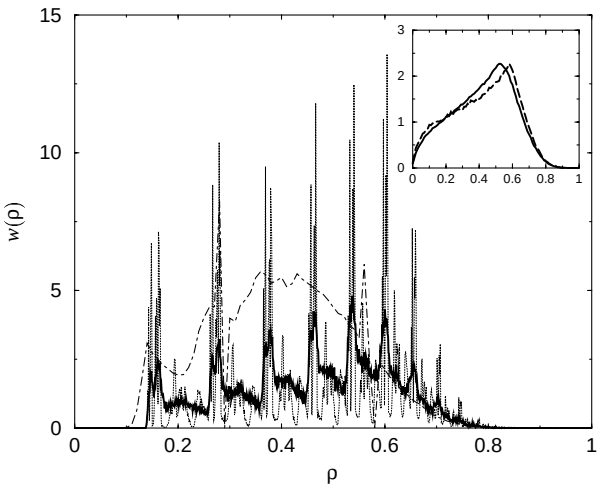

Fig. 10. $w(\rho)$ for systems with the parameters $s_0/L^2 = 0.15$ and $L = 115$ (for the solid line), $L = 1600$ (for the dotted line), $L = 10$ (for the dash-dotted line) The $w(\bar{\rho})$ values for the $L = 10$ system are multiplied by 2. The measured mean tree densities are $\bar{\rho} = 0.454$, 0.455, 0.394. The inset shows $w(\rho)$ for the test simulation with an exponential probability distribution for s_0. The values of L, and the mean value of s_0 are the same as for the solid and dotted curve in the main figure, the measured mean tree densities are $\bar{\rho} = 0.425$ and 0.428.

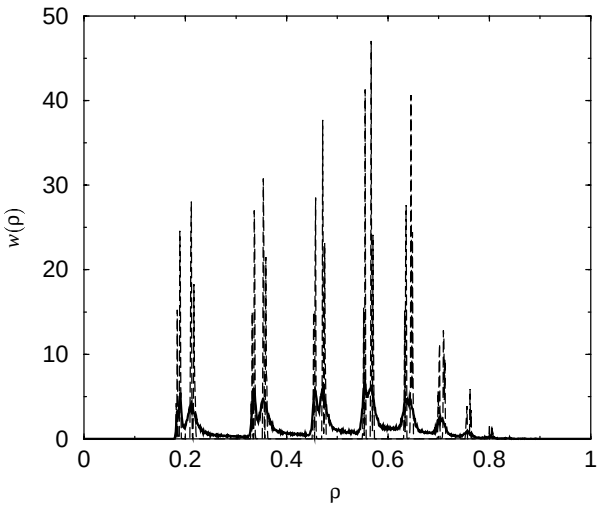

Fig. 11. $w(\rho)$ for systems with the parameters $s_0/L^2 = 0.20$ and $L = 100$ (for the solid line), 1600 (for the dotted line). The measured mean tree densities are $\bar{\rho} = 0.474$, 0.473.

much higher than the percolation occur seldom, explaining the rapid decrease of $w(\rho)$ above the percolation threshold. (c) As the system size increases for fixed $p = s_0/L^2$, there occur peaks in the density distribution which become sharper and more numerous for larger L (Figs. 10 and 11). This can be explained by realizing that the difference between finite and system spanning fires becomes more pronounced as L increases. In the limit $L \to \infty$, finite fires do not affect the density at all, while system spanning fires reduce it to a small value. Subsequent filling events then increase the density to $1 - \exp(-p)$, $1 - \exp(-2p)$, $1 - \exp(-3p)$, etc., until the density is above the percolation threshold and another system spanning fire can occur. These system spanning fires do not always occur at the first instance where the density is above ρ_{perc}, since lightning might strike and empty a site. Also, the density immediately after a system spanning fire depends slightly on the density before the fire. Therefore, the series of density values given above, becomes slightly shifted, depending on the density just before the last system spanning fire. These shifted series of peaks, in turn, give rise to further possible density values above ρ_{perc}, leading to an additional series of peaks, etc. This is the mechanism leading to the fractal peak structure that emerges as L is increased. For smaller

L, the effect of small fires leads to a larger width of the peaks, which can therefore not be resolved when they are close together.

As mentioned in the introduction, the peaks in $w(\rho)$ are due to the fact that lightning can strike the system only between two filling steps. Had we instead performed our simulations using a small tree growth probability p and a small lightning probability f, lightning could strike the system between the growth of any two trees. However, such a simulation would be very slow. In order to make sure that our choice of the algorithm has no other effect on the results apart from the peaks in $w(\rho)$, we performed a test simulation where s_0 is not the same for each filling step. For each filling step, we chose s_0 randomly from an exponential distribution $P(s_0) = (L^2p)^{-1}\exp(-s_0/(L^2p))$. Such an exponential distribution results when lightning can strike the system between the growth of any two trees with the same probability. The mean number of trees growing between two lightning strokes is now smaller than before. The reason is that the majority of filling steps increase the tree number by a value smaller than L^2p, and that during large filling events the tree density becomes high and most of the sites chosen for filling are already occupied. The mean tree densities evaluated according to equation (4) are consequently slightly smaller than before.

The probability density $w(\rho)$ for the tree density resulting from this modified algorithm is shown in the insets in Figures 9 and 10. As expected, the peaks have vanished, while the change in shape from a curve with peak around 0.4 to a curve with peak near 0.6 due to finite-size effects is the same as before.

4 Conclusion

In this paper, we have studied finite-size effects in the SOC forest-fire model. As these effects become stronger, the system rearranges from a structure with patches of different densities to a more homogeneous structure with large density fluctuations in time. This rearrangement is reflected in the structure of the fire size distribution, in the mean tree density, and in the temporal density fluctuations. Qualitatively similar (although quantitatively different) rearrangements are observed when smaller and smaller sections of a large SOC system are studied. Due to these qualitative changes, conventional finite-size scaling does not hold. Our work thus demonstrates that concepts from equilibrium critical phenomena cannot be taken over to the study of SOC systems such as the forest-fire model. Instead, these nonequilibrium critical systems show generically new features unknown in equilibrium. As the scaling ansatz equation (2) which is based on a single length scale $\xi \sim s_0^{\nu}$ can only be approximately correct, the true asymptotic scaling behaviour of the model is still an open question.

We suggest that the reason for the unconventional behaviour of the SOC forest-fire model is the fact that two qualitatively different types of fires occur: those that burn down a patch of high tree density of fractal dimension 2, and those that burn down a tree cluster of a smaller fractal dimension within a region of a tree density below the percolation threshold. As a consequence, the scaling behaviour of the system cannot be characterized using only one length scale. While the superposition of the two types of fires creates the impression of simple scaling as long as finite-size effects are small, the difference between them becomes clearly visible for smaller system sizes, where system spanning fires receive a larger weight. We suggest that the superposition of the two types of fires is also responsible for the other unconventional features of the SOC forest-fire model listed in the introduction.

Models related to the present one have been studied in [8,25] and [7]. In these models, the tree density is globally conserved by filling exactly the same number of trees into the system that have been burnt. As long as the density is below the critical value, these models are equivalent and show the critical behaviour of the SOC forest-fire model as the critical density is approached from below. They were introduced for the purpose of studying the SOC forest-fire model beyond the critical point, *i.e.* for densities larger than the critical density $\bar{\rho}_c$. As the density increases beyond the critical density, both models undergo large-scale rearrangements. In [8,25], where trees are refilled only after the end of a fire, the new structure consists of a finite number of large domains of different density. In [7], where each tree is refilled into the system immediately after it is burnt, the new structure has a continuously burning fire, and resembles the forest-fire model without lightning introduced earlier by Bak, Chen, and Tang [26], which shows spiral-shaped fire fronts [27]. In both these models, the dynamics in the restructured state are dominated by large fires burning forests of a fractal dimension two, similarly to the restructuring due to finite-size effects reported in this paper.

Let us conclude by noting that it is unclear whether the behaviour in higher dimensions resembles that in two dimensions. Clearly, as long as the "patchy" structure with two qualitatively different types of fire occurs, mean-field theory which neglects all spatial structure [17–19] cannot apply, and the system must be below its upper critical dimension. The recent paper by Bröker and Grassberger [28] on the forest-fire model without lightning indicates that unusual scaling behaviour can occur also in 3- and 4-dimensional forest-fire models. If 6 is the upper critical dimension of the forest-fire model, as suggested in [3,17,18], then the scaling behaviour of the forest-fire model should be conventional above 6 dimensions.

This work was supported by EPSRC Grant GR/K79307, and by the EU network project (TMR) "fractal structures and self organization", EU-contract ERPFMRXCT980183.

References

1. P. Bak, C. Tang, K. Wiesenfeld, Phys. Rev. Lett. **59**, 381 (1987); Phys. Rev. A **38**, 364 (1988); P. Bak, M. Creutz, in *Fractals in Science*, edited by A. Bunde, S. Havlin (Springer, Berlin, 1994).

2. B. Drossel, F. Schwabl, Phys. Rev. Lett. **69**, 1629 (1992).
3. S. Clar, B. Drossel, F. Schwabl, Phys. Rev. E **50**, 1009 (1994).
4. Z. Olami, H.J.S. Feder, K. Christensen, Phys. Rev. Lett. **68**, 1244 (1992).
5. K. Sneppen, P. Bak, Phys. Rev. Lett. **71**, 4083 (1993); M. Paczuski, S. Maslov, P. Bak, Phys. Rev. E **53**, 414 (1996).
6. D. Sornette, A. Johansen, I. Dornic, J. Phys. I France **5**, 325 (1995).
7. S. Clar, K. Schenk, F. Schwabl, Phys. Rev. E **55**, 2174 (1997).
8. S. Clar, B. Drossel, F. Schwabl, Phys. Rev. Lett. **75**, 2722 (1995).
9. A. Honecker, I. Peschel, Physica A **239**, 509 (1997).
10. B. Drossel, Phys. Rev. Lett. **76**, 936 (1996).
11. The same result is also found in the most recent unpublished simulations by K. Schenk.
12. B.D. Malamud, G. Morein, D.L. Turcotte, Science **281**, 1840 (1998).
13. S. Clar, B. Drossel, F. Schwabl, J. Phys. C **8**, 6803 (1996).
14. C. Tebaldi, M. De Menech, A.L. Stella, Phys. Rev. Lett. **83**, 3952 (1999); B. Drossel, Phys. Rev. E **61**, R2171 (2000).
15. P. Grassberger, J. Phys. A **26**, 2081 (1993).
16. C.L. Henley, Phys. Rev. Lett. **71**, 2741 (1993).
17. K. Christensen, H. Flyvberg, Z. Olami, Phys. Rev. Lett. **71**, 2737 (1993).
18. B. Drossel, F. Schwabl, Physica A **204**, 212 (1994).
19. A. Vespignani, S. Zapperi, Phys. Rev. E **57**, 6345 (1998).
20. H. Patzlaff, S. Trimper, Phys. Lett. A **189**, 187 (1994).
21. V. Loreto, L. Pietronero, A. Vespignani, S. Zapperi, Phys. Rev. Lett. **75**, 465 (1995).
22. S. Lübeck, K.D. Usadel, Phys. Rev. E **55**, 4095 (1997).
23. A. Chessa, H.E. Stanley, A. Vespignani, S. Zapperi, Phys. Rev. E **59**, R12 (1999).
24. D. Stauffer, A. Aharony, *Introduction to Percolation Theory* (Taylor and Francis, London, 1992).
25. S. Clar, B. Drossel, K. Schenk, F. Schwabl, Phys. Rev. E **56**, 2467 (1997).
26. P. Bak, K. Chen, C. Tang, Phys. Lett. A **147**, 297 (1990).
27. P. Grassberger, H. Kantz, J. Stat. Phys. **63**, 685 (1991); W. Moßner, B. Drossel, F. Schwabl, Physica A **190**, 205 (1992).
28. H.M. Bröker, P. Grassberger, Phys. Rev. E **56**, R4918 (1997).